

Buffeting response of long suspension bridges to skew winds

Y. L. Xu[†] and L. D. Zhu[†]

*Department of Civil and Structural Engineering, The Hong Kong Polytechnic University,
Hung Hom, Kowloon, Hong Kong, China*

H. F. Xiang[†]

*State Key Laboratory for Disaster Reduction in Civil Engineering, Department of Bridge Engineering,
Tongji University, Shanghai 200092, China*

(Received October 18, 2002, Accepted May 10, 2003)

Abstract. A long suspension bridge is often located within a unique wind environment, and strong winds at the site seldom attack the bridge at a right angle to its long axis. This paper thus investigates the buffeting response of long suspension bridges to skew winds. The conventional buffeting analysis in the frequency domain is first improved to take into account skew winds based on the quasi-steady theory and the oblique strip theory in conjunction with the finite element method and the pseudo-excitation method. The aerodynamic coefficients and flutter derivatives of the Tsing Ma suspension bridge deck under skew winds, which are required in the improved buffeting analysis, are then measured in a wind tunnel using specially designed test rigs. The field measurement data, which were recorded during Typhoon Sam in 1999 by the Wind And Structural Health Monitoring System (WASHMS) installed on the Tsing Ma Bridge, are analyzed to obtain both wind characteristics and buffeting responses. Finally, the field measured buffeting responses of the Tsing Ma Bridge are compared with those from the computer simulation using the improved method and the aerodynamic coefficients and flutter derivatives measured under skew winds. The comparison is found satisfactory in general.

Key words: long suspension bridge, skew wind, buffeting analysis, wind tunnel test, aerodynamic coefficient, flutter derivative, field measurement, Typhoon Sam, comparison

1. Introduction

To meet the economic, social and recreational needs of the community for safe and efficient transportation systems, more and more long suspension bridges have been built throughout the world in recent years. The safety and reliability of long suspension bridges under strong winds thus attract increasing attention. To monitor the health status of the bridges and to collect the field measurement data for the verification of analytical processes used in wind-resistant design, wind and structural health monitoring systems have also been installed in several long span cable-supported bridges (e.g., Lau *et al.* 1998). The recent field measurement data recorded by the “Wind

[†] Professor

And Structural Health Monitoring System" (WASHMS) installed on the Tsing Ma suspension bridge in Hong Kong by the Hong Kong Highways Department during typhoons manifested that mean wind directions often deviated from the normal of the bridge span (Xu *et al.* 2000a). Wind characteristics, including mean wind speed and turbulence intensity, varied along the bridge longitudinal axis.

The analytical method for the prediction of buffeting response of long suspension bridges in the frequencies domain, which originated in the works of Scanlan and Gade (1977), has evolved in the last ten years to include the contributions from multi-modes and inter-modes of vibration, the effects of lateral flutter derivatives, and others (Jones *et al.* 1998, Katsuchi *et al.* 1999, Xu *et al.* 2000b). Though this approach is very sophisticated, it assumes that mean wind is coming at a right angle to the longitudinal axis of the bridge deck. This leads to some technical difficulties in performing a satisfactory comparison of buffeting response between field measurement and analysis. Some efforts have also been made to take skew winds into consideration in the buffeting analysis of bridges (Xie and Tanaka 1991, Kimura and Tanaka 1992), but they were all based on the decomposition approach (cosine or sine rules). Wind tunnel tests (Tanaka and Davenport 1982), however, revealed that the decomposition approach underestimated the buffeting response of bridges under yaw winds, and it might not truly reflect the effects of skew winds on buffeting response.

In this connection, the conventional buffeting analysis of long span suspension bridges in the frequency domain is first improved in this study to take into account skew winds based on the quasi-steady theory and the oblique strip theory in conjunction with the finite element method and the pseudo excitation method. The aerodynamic coefficients and flutter derivatives of a typical oblique strip model of the Tsing Ma suspension bridge deck under skew winds are then measured in a wind tunnel using specially designed test rigs. The field measurement data, which were recorded during Typhoon Sam in 1999 on the Tsing Ma Bridge by the WASHMS, are analyzed to obtain both wind characteristics and bridge buffeting responses. The field-measured buffeting responses of the Tsing Ma Bridge are finally compared with those from the computer simulation using the improved method together with the aerodynamic coefficients and flutter derivatives measured under skew winds and some empirical formulae for aerodynamic admittance functions and cross spectra of wind turbulence.

2. Buffeting analysis of bridge under skew winds

In the improved buffeting analysis, the three-dimensional finite element approach is employed to establish the governing equation of motion of the entire bridge under skew winds. The formulae for the spectral matrix of buffeting forces on bridge deck, towers and cable under skew winds are derived based on the quasi-steady theory and the oblique strip theory. The pseudo-excitation method is then employed to solve the equations of motion in the frequency domain. With the improved method, not only the effects of skew wind but also the effects of multi-mode, inter-mode and spatial-mode can be properly taken into account. Moreover, the interaction between bridge deck and towers and cables can be naturally included.

2.1. Governing equation of motion for buffeting due to skew winds

Under the framework of finite element approach, the governing equation of motion of a long suspension bridge under skew winds can be expressed

$$\mathbf{M}^s \ddot{\Delta}(t) + (\mathbf{C}^s + \mathbf{C}^{se}) \dot{\Delta}(t) + (\mathbf{K}^s + \mathbf{K}^{se}) \Delta(t) = \mathbf{F}^b(t) \quad (1)$$

where \mathbf{M}^s , \mathbf{C}^s and \mathbf{K}^s are, respectively, the $N \times N$ mass, damping and stiffness matrices of the entire bridge; \mathbf{C}^{se} and \mathbf{K}^{se} are, respectively, the $N \times N$ aeroelastic damping and stiffness matrices referring to the bridge under skew winds; $\mathbf{F}^b(t)$ is the buffeting force vector of N dimensions due to skew winds; and $\Delta(t)$ is the global nodal displacement vector of N dimensions.

2.2. Spectral matrix of buffeting forces due to skew winds

When employing the finite element method to describe the vibration problem of a large structure and to derive the spectral matrix of buffeting forces due to skew winds, a set of coordinate systems should be properly established. A global structural coordinate system XYZ should be set up to consider the overall dynamic equilibrium conditions of the structure. A global wind coordinate system $X_u Y_v Z_w$ is required to define the mean wind velocity and turbulent wind components. The two global coordinate systems are then correlated through the global wind yaw angle and inclination. Fig. 1(a) shows a combination of the XYZ -system and the $X_u Y_v Z_w$ -system. The axis X_u is set along the direction of the mean wind \bar{U} . The axis Y_v is parallel to the X - Y plane. The axis Z_w is upward and perpendicular to the axes X_u and Y_v following the right-hand rule. The positive directions of the three axes X_u , Y_v and Z_w represent the positive directions of velocity fluctuations $u(t)$, $v(t)$, and $w(t)$, respectively. The angles β_0 and θ_0 are used to define the global yaw angle and inclination of the mean wind \bar{U} with respect to the XYZ -system.

With the use of the finite element method, a local structural coordinate system xyz , referring to the static equilibrium position of the bridge, is required for each element to define the matrices of elemental mass, stiffness, damping, and loading. Furthermore, the aerodynamic coefficients and flutter derivatives of the bridge components under skew winds are measured through wind tunnel tests, in which wind yaw angle and inclination are often defined with respect to local wind and reference coordinate systems. The measured coefficients are then expressed as the function of local mean wind yaw angle and inclination. Thus, it is necessary to introduce a local reference coordinate qph -system and a local wind coordinate $\bar{q}\bar{p}\bar{h}$ -system. Fig. 1(b) shows two local coordinate systems. The angles $\bar{\beta}$ and $\bar{\theta}$ are used to define the local yaw angle and inclination of the mean wind \bar{U} in the qph -system. The angles $\beta(t)$ and $\theta(t)$ are, respectively, the local yaw angle and

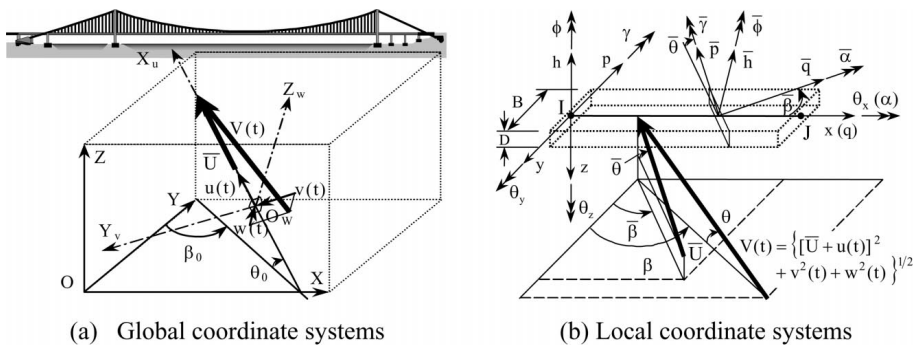


Fig. 1 Global and local coordinate systems

inclination of the transient wind speed $V(t)$ in the qph -system.

It is not difficult to establish the 3×3 transformation matrix \mathbf{T}_{LrGw} from the $X_u Y_v Z_w$ -system to the qph -system. Then, the local yaw angle and inclination $\bar{\beta}$ and $\bar{\theta}$ and their increments $\Delta\beta(t)$ and $\Delta\theta(t)$ in the qph -system can be derived and expressed as follows after a linearization.

$$\bar{\beta} = \sin^{-1}(-t_{11}/\sqrt{t_{11}^2 + t_{21}^2}); \quad \bar{\theta} = \sin^{-1}(t_{31}) \quad (2)$$

$$\Delta\beta(t) = \beta(t) - \bar{\beta} \approx [(t_{11}t_{22} - t_{12}t_{21})/(t_{11}^2 + t_{21}^2)] \frac{v(t)}{\bar{U}} + [(t_{11}t_{23} - t_{13}t_{21})/(t_{11}^2 + t_{21}^2)] \frac{w(t)}{\bar{U}} \quad (3)$$

$$\Delta\theta(t) = \theta(t) - \bar{\theta} \approx (t_{32}/\sqrt{t_{11}^2 + t_{21}^2}) \frac{v(t)}{\bar{U}} + (t_{33}/\sqrt{t_{11}^2 + t_{21}^2}) \frac{w(t)}{\bar{U}} \quad (4)$$

where $\Delta\beta(t)$ and $\Delta\theta(t)$ are the time-dependent increments of the local yaw angle and inclination due to the fluctuations of wind velocity; and t_{ij} is the element of the i -th row and j -th column of the matrix \mathbf{T}_{LrGw} . The aerodynamic forces acting on the structural element due to the transient wind speed $V(t)$ can then be expressed as the function of $\Delta\beta(t)$, $\Delta\theta(t)$, $u(t)$, $v(t)$, $w(t)$, \bar{U} , and the aerodynamic coefficients of the element with respect to $\bar{\beta}$ and $\bar{\theta}$. Finally, by ignoring the non-linear terms of $u(t)$, $v(t)$ and $w(t)$ and performing a series of coordinate transformations, the spectral matrix of the buffeting forces due to skew winds in the global structural coordinate system can be found

$$\mathbf{S}_{FF}^b = \mathbf{P}^{b*}(\omega) \mathbf{S}_{aa}(\omega) \mathbf{P}^{bT}(\omega) \quad (5)$$

where $\mathbf{S}_{aa}(\omega)$ is the spectral matrix of wind fluctuations; $\mathbf{P}^b(\omega)$ is the matrix of the aerodynamic coefficients in a global sense under skew winds. The superscripts “*” and “T” represent the matrix operation of conjugation and transpose, respectively. The expression of $\mathbf{P}^b(\omega)$ can be written as

$$\mathbf{P}^b(\omega) = [\mathbf{T}_1 \mathbf{P}_1^b(\omega), \mathbf{T}_2 \mathbf{P}_2^b(\omega), \dots, \mathbf{T}_m \mathbf{P}_m^b(\omega)] \quad (6)$$

$$\mathbf{P}_i^b(\omega) = \bar{\mathbf{T}}_{GsLs,i} \tilde{\mathbf{N}}_i^T \mathbf{T}_{LsL\bar{w},i} \bar{\mathbf{A}}_i^b(\omega) \quad (7)$$

where m is the number of the total elements on which the buffeting forces need to be accounted; $\bar{\mathbf{A}}_i^b(\omega)$ is the 6×3 matrix of local aerodynamic coefficients of the i th element; $\mathbf{T}_{LsL\bar{w},i}$ is the 6×6 transformation matrix from the local wind coordinates system \overline{qph} to the local structural coordinate system xyz for the i th element; $\tilde{\mathbf{N}}_i$ is the 6×12 matrix of the displacement interpolation functions of the i th element as used in the conventional finite element method; $\mathbf{T}_{GsLs,i}$ is the 12×12 transformation matrix from the local xyz -system to the global XYZ -system for the i th element; and $\mathbf{T}_i (i = 1, \dots, m)$ is the $N \times 12$ matrix with its elements being either zero or unit to locate the matrix $\mathbf{P}_i^b(\omega)$ at the proper position in the global matrix $\mathbf{P}^b(\omega)$. N is the number of the total degrees of freedom of the whole bridge. The matrix $\bar{\mathbf{A}}_i^b(\omega)$ is the function of the air density ρ , the mean wind speed at the center of the element \bar{U}_i , the element width B_i , the aerodynamic coefficients and their derivatives of the element under skew winds, the coordinate transformation matrix \mathbf{T}_{LrGw} , and others. The resulting expression is rather complicated. If the local reference

coordinate system is the same as the global structural coordinate systems, i.e., $\bar{\beta} = \beta_0$ and $\bar{\theta} = \theta_0$, the matrix $\bar{A}_i^b(\omega)$ can be reduced as:

$$\bar{A}_i^b(\omega) = \frac{\rho \bar{U}_i}{2} \begin{bmatrix} 2BC_{C_{\bar{q}}}\chi_{C_{\bar{q}}u} & B(-C_{D_{\bar{p}}} + C_{L_{\bar{h}}}\tan\theta_0 + C'_{C_{\bar{q}}}/\cos\theta_0)\chi_{C_{\bar{q}}v} & BC'_{C_{\bar{q}}}\chi_{C_{\bar{q}}w} \\ 2BC_{D_{\bar{p}}}\chi_{D_{\bar{p}}u} & B(C_{D_{\bar{q}}} + C'_{D_{\bar{p}}}/\cos\theta_0)\chi_{D_{\bar{p}}v} & B(-C_{L_{\bar{h}}} + C'_{D_{\bar{p}}})\chi_{D_{\bar{p}}w} \\ 2BC_{L_{\bar{h}}}\chi_{L_{\bar{h}}u} & B(-C_{C_{\bar{q}}}\tan\theta_0 + C'_{L_{\bar{h}}}/\cos\theta_0)\chi_{L_{\bar{h}}v} & B(C_{D_{\bar{p}}} + C'_{L_{\bar{h}}})\chi_{L_{\bar{h}}w} \\ 2B^2C_{M_{\bar{\alpha}}}\chi_{M_{\bar{\alpha}}u} & B^2(-C_{M_{\bar{\gamma}}} + C_{M_{\bar{\phi}}}\tan\theta_0 + C'_{M_{\bar{\alpha}}}/\cos\theta_0)\chi_{M_{\bar{\alpha}}v} & B^2C'_{M_{\bar{\alpha}}}\chi_{M_{\bar{\alpha}}w}(\omega) \\ 2B^2C_{M_{\bar{\gamma}}}\chi_{M_{\bar{\gamma}}u} & B^2(C_{M_{\bar{\alpha}}} + C'_{M_{\bar{\gamma}}}/\cos\theta_0)\chi_{M_{\bar{\gamma}}v} & B^2(-C_{M_{\bar{\phi}}} + C'_{M_{\bar{\gamma}}})\chi_{M_{\bar{\gamma}}w} \\ 2B^2C_{M_{\bar{\phi}}}\chi_{M_{\bar{\phi}}u} & B^2(-C_{M_{\bar{\alpha}}}\tan\theta_0 + C'_{M_{\bar{\phi}}}/\cos\theta_0)\chi_{M_{\bar{\phi}}v} & B^2(C_{M_{\bar{\gamma}}} + C'_{M_{\bar{\phi}}})\chi_{M_{\bar{\phi}}w} \end{bmatrix}_i \quad (8)$$

where $C_{C_{\bar{q}}}$, $C_{D_{\bar{p}}}$, $C_{L_{\bar{h}}}$, $C_{M_{\bar{\alpha}}}$, $C_{M_{\bar{\gamma}}}$ and $C_{M_{\bar{\phi}}}$ are, respectively, the coefficients of cross, drag, and lift forces and pitching, rolling and yawing moments with respect to the local wind coordinate system. and $qp\bar{h}$. $(\)^{\beta}$ are $(\)^{\theta}$ the partial derivatives of the corresponding coefficients with respect to the yaw angle β and inclination angle θ . $\chi_{fr}(\omega)$ ($f=C_{\bar{q}}, D_{\bar{p}}, L_{\bar{h}}, M_{\bar{\alpha}}, M_{\bar{\gamma}}, M_{\bar{\phi}}; r=u, v, w$) are the 18 aerodynamic admittance functions.

2.3. Aeroelastic stiffness and damping matrices of bridge under skew winds

To determine the aeroelastic stiffness and damping matrices of the entire bridge under skew winds for the governing equation of motion Eq. (1), the aeroelastic stiffness and damping matrices for the k th element in the local structural coordinate xyz -system should be derived first based on the self-excited forces which are often expressed in terms of the Scanlan's flutter derivatives. Since this investigation concerns skew winds, the Scanlan's flutter derivatives are measured from the wind tunnel tests of oblique deck segments under skew winds. Thus, they are not only the function of the reduced frequency but also the function of the local mean wind yaw and inclination. Theoretically, there should be six components of the aeroelastic forces/moments but only the pitching moment $M_{\bar{\alpha}}^{se}$, drag $D_{\bar{p}}^{se}$ and lift $L_{\bar{h}}^{se}$ are generally regarded to be important to the buffeting response prediction of the bridge (Scanlan and Gade 1977). These self-excited forces in the local reference coordinate system can be expressed as

$$f_{r,k}^{se}(\bar{\beta}, \bar{\theta}, K) = A_{S,k}(\bar{\beta}, \bar{\theta}, K)\delta_{Lr,k} + A_{D,k}(\bar{\beta}, \bar{\theta}, K)\delta_{Lr,k} \quad (9)$$

where

$$f_{r,k}^{se} = (M_{\bar{\alpha}}^{se}, D_{\bar{p}}^{se}, L_{\bar{h}}^{se})_k^T \quad (10)$$

$$\delta_{Lr,k} = (\delta_{\alpha}, \delta_p, \delta_h)_k^T, \quad \delta_{Lr,k} = (\delta_{\alpha}, \delta_p, \delta_h)_k^T \quad (11)$$

$$\mathbf{A}_{S,k}(\bar{\beta}, \bar{\theta}, K) = \frac{1}{2} \rho \bar{U}^2 K^2 \begin{bmatrix} B^2 A_3^* & BA_6^* & BA_4^* \\ BP_3^* & P_4^* & P_6^* \\ BH_3^* & H_6^* & H_4^* \end{bmatrix}_{(\bar{\beta}, \bar{\theta}, K)} \quad (12)$$

$$\mathbf{A}_{D,k}(\bar{\beta}, \bar{\theta}, K) = \frac{1}{2} \rho \bar{U} BK \begin{bmatrix} B^2 A_2^* & BA_5^* & BA_1^* \\ BP_2^* & P_1^* & P_5^* \\ BH_2^* & H_5^* & H_1^* \end{bmatrix}_{(\bar{\beta}, \bar{\theta}, K)} \quad (13)$$

where $\delta_p(t)$ and $\delta_h(t)$ are the dynamic displacements along the axis p and the axis h and $\delta_\alpha(t)$ is the dynamic angular displacement about the axis q ; each over-dot denotes one order of partial differentiation with respect to time; B is the characteristic width of the true cross section of the bridge segment; $K=B\omega/\bar{U}$ is the reduced frequency; ω is the circular frequency; and $P_i^*(\bar{\beta}, \bar{\theta}, K)$, $H_i^*(\bar{\beta}, \bar{\theta}, K)$ and $A_i^*(\bar{\beta}, \bar{\theta}, K)$ ($i=1, \dots, 6$) are the flutter derivatives of the oblique bridge segment and they are the function of the local mean wind yaw angle $\bar{\beta}$ and inclination $\bar{\theta}$ as well as the reduced frequency K or the reduced velocity $2\pi/K$. It should be noted that the above aeroelastic pitching moment M_α^{se} , drag D_p^{se} , and lift L_h^{se} refer to the local reference coordinate qph -system of the bridge deck segment though the flutter derivatives are measured from the oblique segment. These are consistent with the motions of the bridge deck as well as the wind tunnel measurements of flutter derivatives described in the next section.

By using the principle of virtual work and the coordinate transformation matrices, the aeroelastic stiffness and damping matrices for the element in the local structural coordinate xyz -system can be first found from the self-excited forces in Eq. (9) in the local reference coordinate system. The aeroelastic stiffness and damping matrices for the element in the local structural coordinate xyz -system can then be transformed to the global structural coordinate XYZ -system. Finally, the global aeroelastic stiffness and damping matrices in Eq. (1) in the global structural coordinate system can be obtained by assembling the aeroelastic stiffness and damping matrices for all the elements in the same way as the assemblage of the global structural stiffness and damping matrices from the elemental structural stiffness and damping matrices. The information on the application of the pseudo-excitation method to find the solution of Eq. (1) can be referred to Sun *et al.* (1999).

3. Aerodynamic coefficients and flutter derivatives of bridge deck under skew winds

To carry out the comparison of buffeting response of the Tsing Ma suspension bridge under skew winds between field measurement and analysis, the aerodynamic coefficients and flutter derivatives of the bridge deck under skew winds have to be measured through wind tunnel tests. Thus, the special test rigs and the models of a typical deck section were designed. The tests were carried out in the TJ-2 Wind Tunnel of the State Key Laboratory for Disaster Reduction in Civil Engineering at Tongji University, Shanghai. The following is only a brief description to the wind tunnel tests in order to facilitate the understanding of this systematic study. The detail information on the design of sectional models, the development of test rigs and measurement systems, and the analysis of test results can be found in Zhu *et al.* (2002a, 2002b).

3.1. Aerodynamic coefficients of bridge deck under skew winds

Different from traditional wind tunnel tests for measuring aerodynamic coefficients of a bridge deck under normal wind, a sectional model of parallelogram was used in this study to measure aerodynamic coefficients of a bridge deck under skew winds. The oblique sectional model was installed vertically in the wind tunnel (see Fig. 2). The geometric scale of the deck sectional model of the Tsing Ma Bridge was set as 1:100. To avoid 3D flow effects around the two ends of the oblique sectional model, two surrounding segments (the upper segment and the lower segment) were introduced and each was mounted close to one end of, but free from any touch to, the sectional model (the measured segment). To accommodate a few yaw angles in the test using one sectional model, two adjustable parts were designed and placed between the top part and the middle part and between the bottom part and the middle part of the model separately. Each adjustable part consisted of four small triangle wedges used to adjust the middle part to form the upper and lower surrounding segments for five designated yaw angles ($\bar{\beta}=0^\circ, 5^\circ, 13^\circ, 20^\circ$ and 31°). The bottom part of the model was mounted rigidly on the turning table of the wind tunnel through a special apparatus that could be adjusted to meet the desired yaw angle. The desired angle of inclination was realized by rotating the turning table. To enrich the database for generating curves of aerodynamic coefficients, it was decided that the model was tested under a wide combination of yaw angles from 0° to 34° at an interval of 1° or 2° and inclined angles from -10° to $+10^\circ$ at an interval of 1° . For the other mean wind yaw angles around one of the five major yaw angles, only the model was adjusted to the targeted mean wind yaw angle while the model end angle remains unchanged.

The six aerodynamic forces/moments applied on the test segment were measured by a force balance of six components. The tests were carried out under a mean wind of 15 m/s. The measured forces/moments were then used to calculate the aerodynamic coefficients with respect to the local wind coordinates \overline{qph} and the true width of the cross section. Fig. 3 shows the results at a yaw

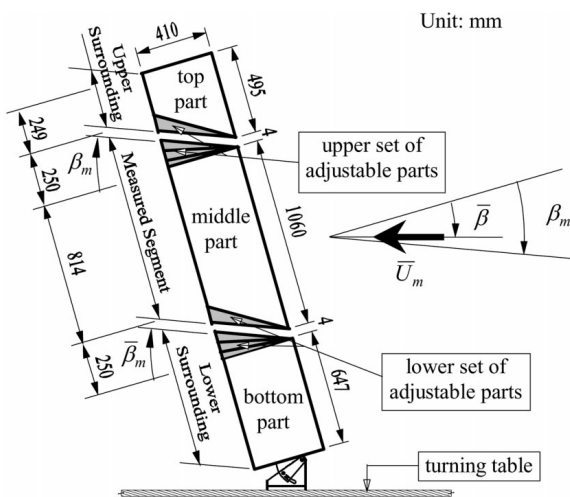


Fig. 2 Configuration of deck sectional model for aerodynamic coefficient measurement

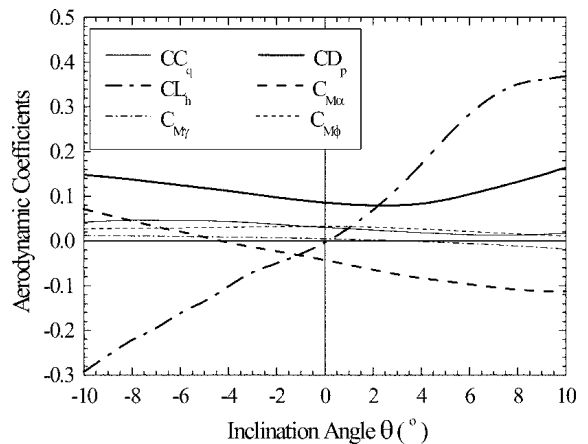


Fig. 3 Effects of inclination on aerodynamic coefficients

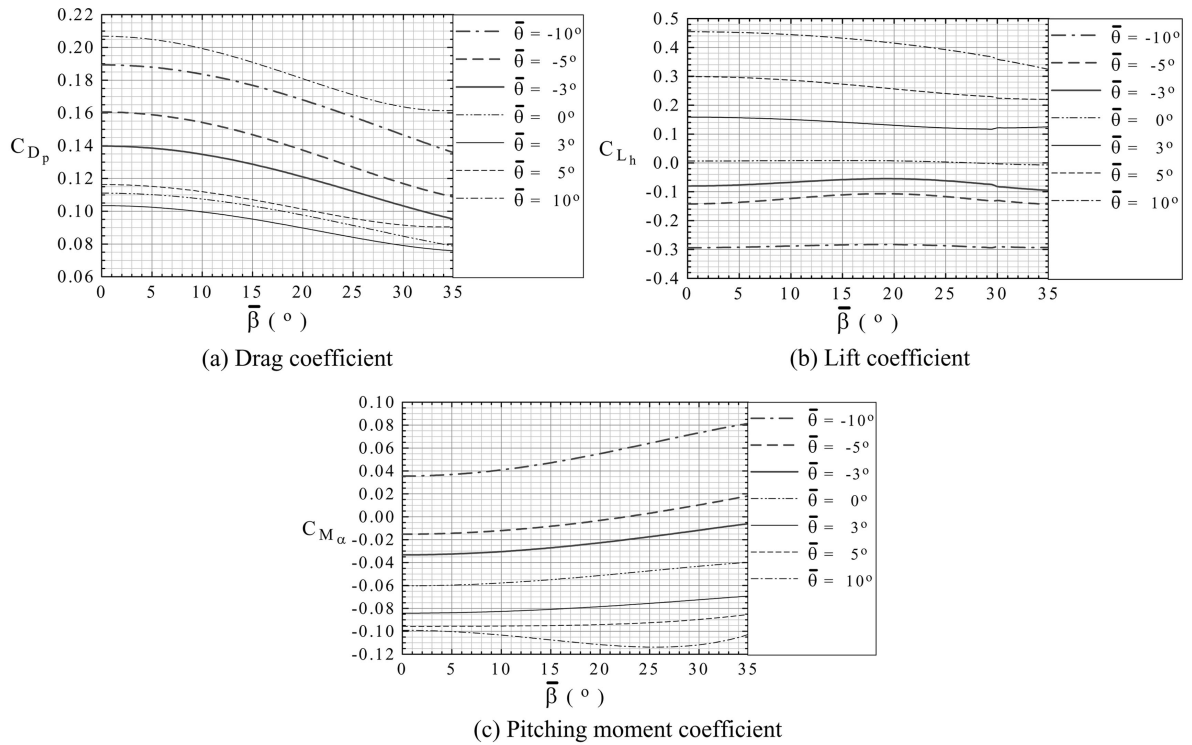


Fig. 4 Effects of yaw angle on aerodynamic coefficients

angle of 29.15° obtained by the curve fitting and proper interpolation of the measured data. Fig. 4 displays variations of drag, lift, and pitching moment coefficients with yaw angle. It was found from the measured results that the drag, lift, and pitching moment coefficients were much larger than the crosswind force, rolling moment, and yawing moment coefficients even at a large yaw angle of 31° . It is seen from Fig. 4 that the variation of lift coefficient with yaw angle is small. The value of drag coefficient, however, decreases with increasing yaw angle whereas the value of pitching moment increases with increasing yaw angle. It was also found that the coefficients of aerodynamic forces along the model axes p and h , and aerodynamic moment around the model q -axis did not comply with the traditional cosine rule, particularly for large yaw angle cases.

3.2. Flutter derivatives of bridge deck under skew winds

To facilitate the investigation of flutter derivatives of the bridge deck under skew winds, the dynamic sectional deck model was designed as an oblique strip composed of five major parts: one middle part, two end parts, and two support arms between the middle and end parts. The length of the middle part was 2.407 m for a 1/100 geometric scale and it remained unchanged in all the tests. The two end parts of the model were trapezoidal and its length changed with yaw angle designated. The two ends of the model were always kept in parallel to the incident wind in the wind tunnel for different wind yaw angles. The oblique sectional model was suspended in the wind tunnel with eight helical springs via the two support arms as shown in Fig. 5.



Fig. 5 Test model for flutter derivative measurement

The test sectional model simulated the 1st symmetric vertical bending mode of vibration and the 1st symmetric torsional mode of vibration of the Bridge (Xu *et al.* 1997). The coupled 2DOF free decay vibration was performed to identify the eight Scanlan's flutter derivatives A_i^* and H_i^* ($i=1,2,3,4$) in conjunction with the unifying least square method (Gu *et al.* 2000). Seven model inclinations ($\bar{\theta}=0^\circ, \pm 2^\circ, \pm 3^\circ, \pm 5^\circ$) and five yaw angles ($\bar{\beta}=0^\circ, 5^\circ, 13^\circ, 20^\circ, 31^\circ$) were considered, resulting in a total of 35 cases with respect to the model position. For each given position, the model was given a series of coupled 2DOF free vibrations corresponding to a series of wind speeds to obtain flutter derivative curves as a function of reduced velocity.

The test data of flutter derivatives for a given model position were interpolated/extrapolated and fitted to generate the design curves of eight flutter derivatives H_i^* and A_i^* ($i=1,2,3,4$). Fig. 6 shows the flutter derivative A_2^* measured at an inclination $\bar{\theta}=5^\circ$ for yaw angles $\bar{\beta}=0^\circ, \bar{\beta}=5^\circ, \bar{\beta}=13^\circ, \bar{\beta}=20^\circ$, and $\bar{\beta}=31^\circ$. Fig. 7 depicts the flutter derivatives H_4^* measured at an inclination $\bar{\theta}=3^\circ$ for yaw angles $\bar{\beta}=0^\circ, \bar{\beta}=5^\circ, \bar{\beta}=13^\circ, \bar{\beta}=20^\circ$, and $\bar{\beta}=31^\circ$. It was found from the measured results that

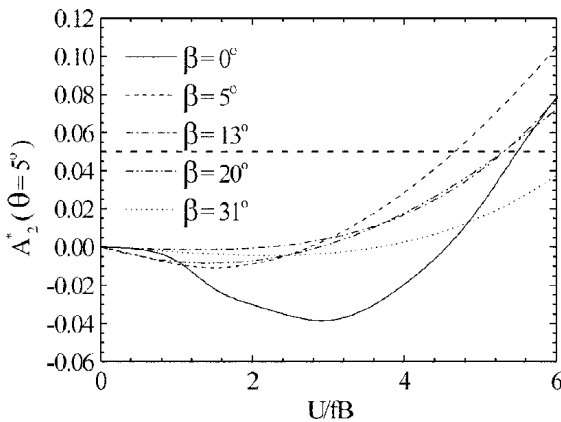


Fig. 6 Flutter derivative curves A_2^*

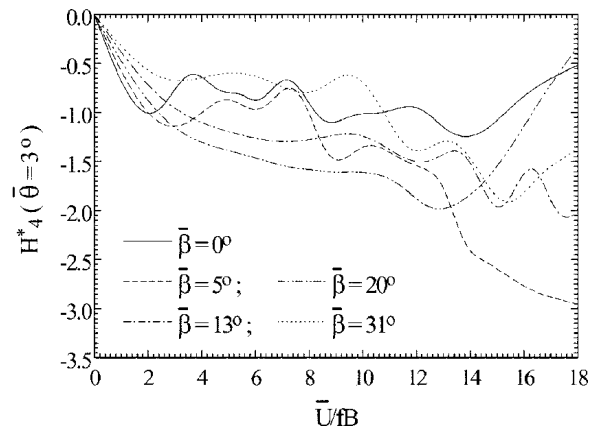


Fig. 7 Flutter derivative curves (H_4^*)

the effects of wind yaw angle on the flutter derivatives H_1^* , H_2^* , H_3^* , A_2^* and A_3^* were in general not conspicuous in the range of lower reduced velocity, but became considerable in the range of higher reduced velocity. The flutter derivatives H_4^* , A_1^* and A_4^* , however, oscillated remarkably with reduced velocity and were affected by yaw angle within the whole range of reduced velocity. The critical wind speed of the Tsing Ma Bridge might not increase with increasing wind yaw angle. For example, based on the single-degree-of-freedom torsional flutter theory, the results presented in Fig. 6 indicate that the lowest critical wind speed takes place first at $\bar{\beta}=5^\circ$ and then $\bar{\beta}=20^\circ$, 13° , 0° , and 31° in an ascending order. This means that the lowest critical wind speed could occur when mean wind deviated from the normal of the bridge axis. It was also found that major flutter derivatives estimated by the empirical formulae based on the skew wind theory (Scanlan 1999) deviated considerably from the measured results (Zhu *et al.* 2002b).

4. Field measurements of Tsing Ma Bridge during Typhoon Sam

4.1. Tsing Ma Bridge and WASHMS

The Tsing Ma Bridge in Hong Kong is the longest suspension bridge in the world carrying a dual three-lane highway on the upper level of the bridge deck and two railway tracks and two carriageways on the lower level within the bridge deck. The alignment of bridge deck deviates from the east-west axis for about 17° in anti-clockwise. The typical section of the bridge deck is 41 m wide and 7.643 m high. The two bridge towers of 206 m high are made of pre-stressed concrete. The east bridge tower sits on the northwest shoreline of Tsing Yi Island, called the Tsing Yi tower while the west bridge tower sits on Ma Wan Island, called the Ma Wan tower (see Fig. 8).

To monitor the health status of the Tsing Ma Bridge, a instrumentation system called the Wind And Structural Health Monitoring System (WASHMS) was installed in the bridge by the Hong Kong Highways Department (Lau *et al.* 1998). The WASHMS has seven types of sensors including six sets of anemometer and 24 uni-axial servo type accelerometers. Two digital ultrasonic anemometers (AneU), called Gill Wind Master Ultrasonic Anemometer, were installed on the north

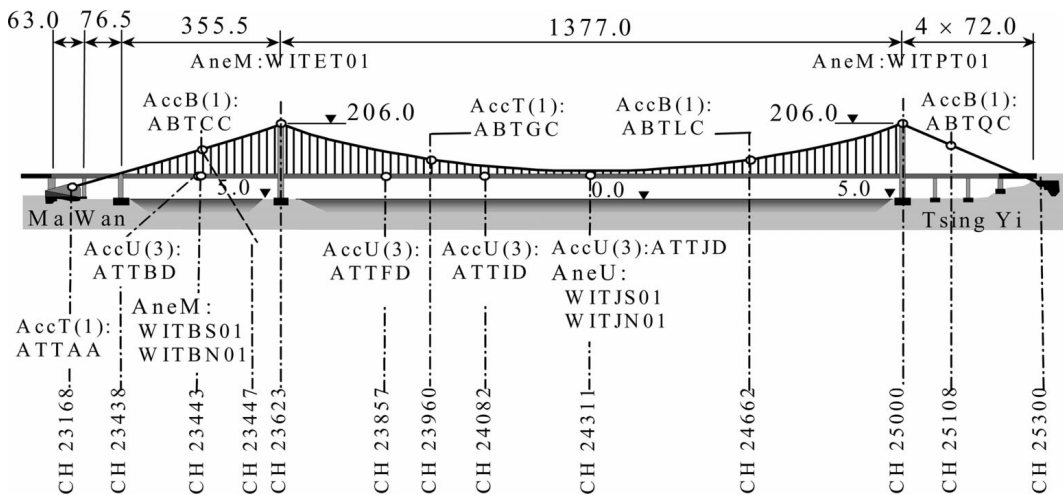


Fig. 8 Locations of anemometers and accelerometers

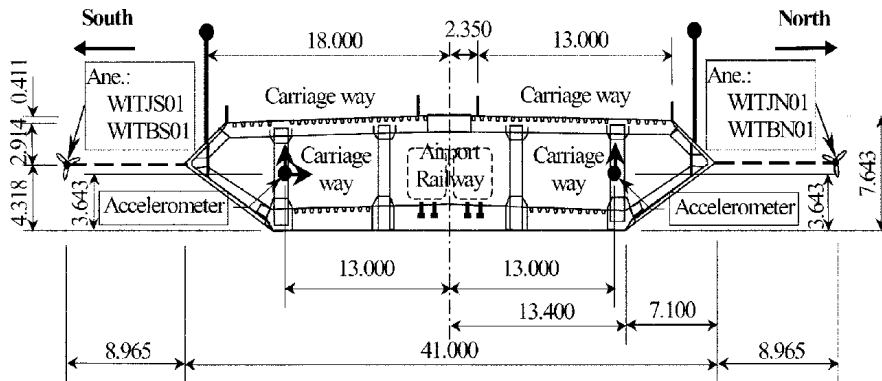


Fig. 9 Positions of sensors on cross section of bridge deck

side and south side, respectively, of the bridge deck at the middle main span (75.314 m in elevation). They are specified as WITJN01 and WITJS01 in Figs. 8 and 9. Each ultrasonic anemometer can measure three components of wind velocity simultaneously. Two analogue mechanical anemometers (AneM) were located at two sides of the bridge deck near the middle of the Ma Wan side span (62.944 m in elevation), specified as WITBN01 at the north side and WITBS01 at the south side in Figs. 8 and 9. Each analogue mechanical anemometer consists of a horizontal component, called RM YOUNG 05106 Horizontal Anemometer, and a vertical component, named as RM YOUNG 27106 Vertical Anemometer. Another two analogue mechanical anemometers (AneM) of horizontal component only were arranged over the top of each bridge tower (217.084 m in elevation). They are specified as WITPT01 for the Tsing Yi tower and WITET01 for the Ma Wan tower in Fig. 8.

The servo-type accelerometers are of the brand Allied Signal Aerospace Q-Flex QA700. As shown in Fig. 8, three different types of arrangement for acceleration measurement are used in the system. AccT represents the Tri-axial measurement by using three uni-axial accelerometers assembled perpendicularly to each other, which was mounted at the position ABTGC on the south-cable and at the position ATTAA on the Ma Wan Anchorage. AccB indicates the Bi-axial measurement by using two uni-axial accelerometers assembled perpendicularly to each other, which was installed at the south-cable positions ABTCC, ABTLC and ABTQC. AccU means the Uni-axial measurement by using only one accelerometer to give signal in one prescribed direction. A total of 12 uni-axial accelerometers are used in AccU measurement, which was arranged at the four deck sections (ATTID, ATTJD, ATTFD and ATTBDD). At each section, there are two accelerometers, horizontally separated with 13 m, measuring acceleration in the vertical direction and one accelerometer measuring acceleration in the lateral direction, as shown in Fig. 9.

4.2. Typhoon Sam

After developed at about 680 km east-northeast of Manila on 19 August 1999, the tropical depression Sam moved west-northwestwards over the Pacific and intensified into a tropical storm at that night. It then moved north-westly towards the coast of Guangdong and became a typhoon on a late morning of 22 August near Hong Kong. Typhoon Sam finally made landfall over the eastern part of Sai Kung in Hong Kong at around 6 p.m. on 22 August. Following landfall, Sam traversed the northeastern part of the New Territories at a speed of about 25 km/h and crossed into Shenzhen,

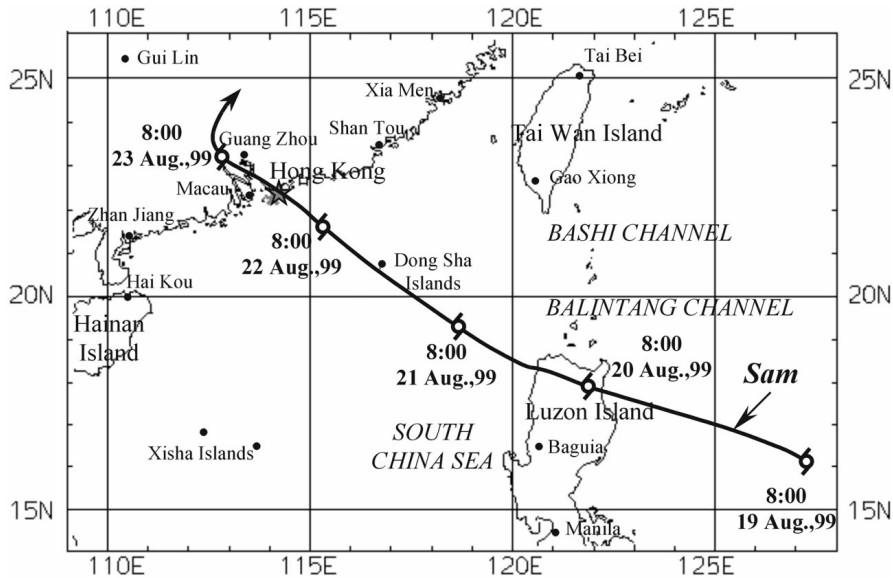


Fig. 10 Tracks of typhoon sam

and then weakened gradually over inland Guangdong on 23 August (see Fig. 10). Hong Kong Observatory recorded a maximum hourly-mean wind speed of about 27 m/s and a maximum gust wind speed of about 41 m/s at a 75 m height at Waglan Island during the passage of Typhoon Sam. The lowest instantaneous pressure at mean sea level was recorded as 979.0 hPa.

The WASHMS timely recorded wind velocity and bridge buffeting responses. The sampling frequency for wind velocity was 2.56 Hz and the cut-off frequency was 1.28 Hz. The sampling frequency of acceleration response was 25.6 Hz and the cut-off frequency was 12.8 Hz.

4.3. Measured wind data

After a careful examination of all the measured wind velocity time histories, one-hour record of wind velocity between 14:11 to 15:11 Hong Kong Time (HKT) on 22 Aug. 1999 was selected for the analysis. During this period, incident wind blew to the Tsing Ma Bridge from the direction near to the north. Therefore, the wind data recorded by the anemometers at the south side of the bridge deck were contaminated by the bridge deck itself and were not suitable for the analysis of natural wind structures. Due to the technical reason, the mechanical anemometers installed at the deck and the top of the towers failed to record the wind azimuth. As a result, wind characteristics of Typhoon Sam surrounding the bridge could be extracted only from the wind speed time histories recorded by the three-component ultrasonic anemometer installed on the north side of the bridge deck at the mid-span. By analyzing the three components of the recorded wind velocity, it was found that the hourly-mean wind speed was about 17.1 m/s and the mean wind blew from north-northeast. The global hourly-mean wind yaw angle β_0 and inclination θ_0 were, respectively, -29.15° and 2.25° . The time histories of fluctuating wind speeds $u(t)$, $v(t)$ and $w(t)$ in the longitudinal (along-wind), lateral, and upward directions were also extracted from the measured three components of wind velocity. It was found that the turbulence intensities were about 18.6%, 20.4% and 14.5%, for $u(t)$,

$v(t)$ and $w(t)$, respectively, and the corresponding integral scales of turbulence were 228 m, 116 m, and 84 m based on the Taylor's hypothesis. The spectral analysis was performed to find the one-side normalized auto spectra of fluctuating wind speeds $u(t)$, $v(t)$ and $w(t)$. The co-spectra and quadrature spectra between every two of the three fluctuating wind speeds were also analyzed. The curve fitting of non-linear least squares was carried out for all the measured spectra.

4.4. Measured bridge acceleration responses

To be consistent with wind analysis, only the acceleration response data recorded from 14:11 to 15:11 HKT on 22 August 1999 were analyzed. They included the lateral, vertical and torsional

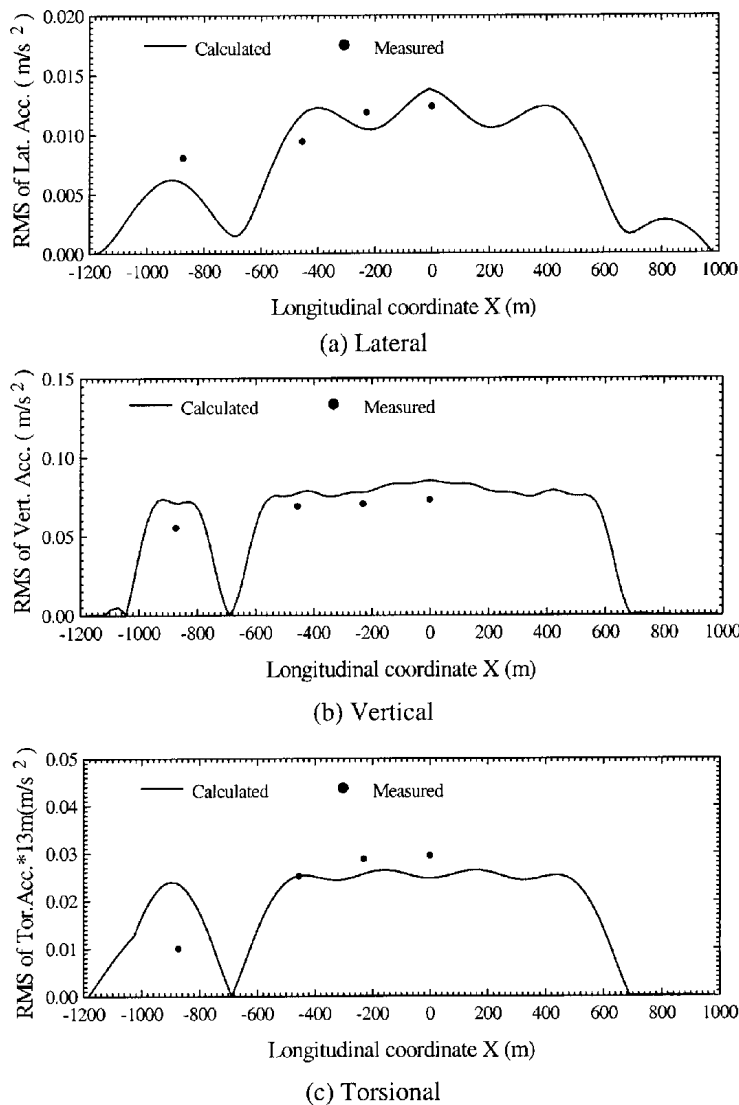


Fig. 11 Comparison between measured and computed RMS acceleration responses of bridge deck

accelerations at the three deck sections in the main span (ATTJD, ATTID and ATTFD) and one deck section in the Ma Wan side span (ATTBD). They also included the lateral and vertical acceleration responses at the four cable sections (ABTQC, ABTLC, ATTGC, and ABTCC) and the longitudinal acceleration response at ATTGC. It is noted that when computing the buffeting response of the Tsing Ma Bridge in the frequency domain, a lower bound and an upper bound of frequency should be set. This depends on how many modes of vibration should be included in the computation and what is the valid frequency range for flutter derivatives obtained from wind tunnel tests. In this study, the upper bound of frequency used in the computation was 0.75 Hz, which is higher than the 45th natural frequency (0.7062 Hz) of the bridge. The lower bound of frequency used in the computation was set as 0.025 Hz because the flutter derivatives measured from the wind tunnel are available only for the reduced velocity lower than 18, namely, only for the frequency

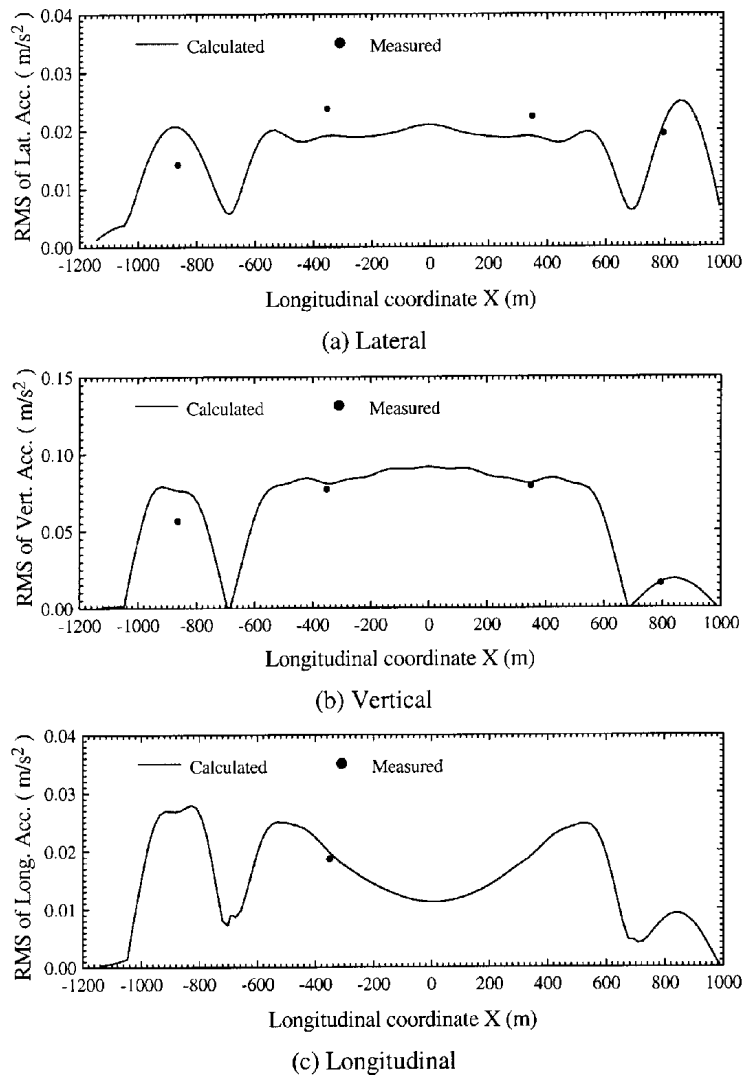


Fig. 12 Comparison between measured and computed RMS acceleration responses of bridge cable

higher than 0.0232 Hz when the mean wind speed is 17.1 m/s and the deck width is 41 m. Therefore, to have a reasonable comparison between computed and measured buffeting responses, the measured response time histories should go through a digital bandpass filter with the same lower and upper bounds of frequency used in the computation. The RMS acceleration responses were then calculated using the filtered response time histories. The resulted root mean square (RMS) acceleration responses are plotted in Fig. 11 for the bridge deck and in Fig. 12 for the bridge cable. The Hilbert-Huang transform (HHT) method was used to identify the modal damping ratios from the measured acceleration responses (Chen *et al.* 2002). The first modal damping ratio of the Bridge was found to be 1.0% in the lateral motion, 2.2% in the vertical motion, and 0.44% in the torsion.

5. Comparison between computed and measured buffeting responses

5.1. Input data

To perform a comparison between the measured and computed buffeting responses of the Tsing Ma Bridge, the buffeting response of the Tsing Ma Bridge under skew wind during Typhoon Sam between 14:11 to 15:11 HKT on 22 August, 1999 was computed using the analytical method proposed in this study. The first 45 modes of vibration of the Bridge were included in the buffeting analysis. The modal damping ratios identified from the measured response time histories were used. The measured mean wind speed of 17.1 m/s at the elevation of 75.314 m with the global yaw angle of -29.15° and the global inclination of 2.25° were used as input wind parameters. The mean wind speed and direction were considered to be uniform along the bridge deck in the computation. According to the Hong Kong code of practice on wind effects, the power law with the exponent of 0.33 was adopted to describe the mean wind profile. The auto-spectra and the cross-spectra of three fluctuating wind speed components were taken as the fitted curves to the measured spectra. The friction velocity u_* was estimated as 1.69 m/s from the measured horizontal shear stress. The exponential decay coefficients for the determination of the root-coherence functions could not be estimated from the field measurement and were taken as those suggested by Simiu and Scanlan (1996). The phase spectra were also not available and thus they were taken as zero.

The aerodynamic coefficients of the bridge deck, tower legs, and tower transverse beams measured from the wind tunnel tests under yaw winds were used in the buffeting analysis. As for the coefficients of drag and crosswind forces of the main cables under skew winds, the formulae based on the traditional cosine rule were employed in the analysis. The aerodynamic forces on the bridge hangers (suspenders) were neglected because they were very small. To include the effects of aeroelastic forces in the buffeting analysis, the eight flutter derivatives of the bridge deck measured under skew winds were used in the computation. The flutter derivatives of P_1^* , P_3^* , P_5^* , H_5^* and A_5^* were not available from the wind tunnel tests and hence the formulae based on the quasi-steady theory were employed in the analysis. The rest five flutter derivatives were considered insignificant to the bridge buffeting response and neglected in the computation. Furthermore, there were no measurement data available on the aerodynamic admittance functions of the Tsing Ma Bridge. The empirical formulae and other measures had to be used. For the bridge tower components including tower legs and transverse beams, the aerodynamic admittance functions were set to unity. For the main cables, the formula suggested by Vickery (1966) for the aerodynamic admittance function of circular cylinder was used. For the bridge deck, the aerodynamic admittance functions proposed by

Davenport (1962) were employed for the 9 aerodynamic admittance functions associated with the drag, crosswind force, and yawing moment of the bridge deck. The other 9 admittance functions associated with the lift, pitching moment, and rolling moment were set to unity.

5.2. Comparison of acceleration response of bridge deck

From the computed acceleration response spectra of the bridge deck, the RMS acceleration responses of the bridge deck could be obtained by the integration of the spectra in the frequency domain. The frequency range for the integration was from 0.025 Hz to 0.75 Hz in order to have a fair comparison. The computed RMS acceleration responses of the bridge deck are plotted in Fig. 11 for the lateral, vertical, and torsional vibrations, respectively. The RMS acceleration responses measured at the four specified deck sections are also plotted in Fig. 11 for the comparison. The measured RMS acceleration responses were directly obtained from the measured acceleration time histories rather than the integration of the power spectra but the bandpass filter was applied between 0.025 Hz and 0.75 Hz to have a fair comparison.

It is seen from Fig. 11 that for the main span, the computed RMS acceleration responses of the bridge deck in the lateral, vertical and torsional directions all are close to the measured results. The relative differences are less than 25%. For the Ma Wan side span, the computed RMS acceleration responses in the lateral and vertical directions are also close to the measured ones, but for the torsional vibration the relative difference between the computed and measured RMS response is as high as 139%.

5.3. Comparison of acceleration response of bridge cable

The comparison between the computed and measured RMS acceleration responses of the main cable is shown in Fig. 12 for the lateral, vertical, and longitudinal vibration, respectively. A good agreement is seen between the computed and measured RMS acceleration responses for the vertical and longitudinal vibration of the cable in the main span and for the lateral and vertical vibration of the free cable in the Tsing Yi side span. The relative differences between the computed and measured RMS responses are less than 8.1%. For the lateral acceleration of the main span cable, the computed RMS acceleration responses also agree with the measured results with the differences less than 20%. However, for the cable section ABTCC in the Ma Wan side span, the differences between the computed and measured RMS responses are significant for both the lateral and vertical vibrations with the relative differences of 46.3% and 35.1%, respectively. This trend is consistent with the comparative results of the bridge deck.

6. Concluding remarks

In this study, wind structures and buffeting responses measured by the Wind and Structural Health Monitoring System (WASHMS) installed on the Tsing Ma Bridge during Typhoons Sam were analyzed. An improved frequency-domain method for buffeting analysis of long suspension bridges under skew winds was presented. A series of wind tunnel tests were performed to measure the aerodynamic coefficients and flutter derivatives of the bridge deck under skew winds using innovative test rigs developed for this study. The comparison of buffeting response of the Tsing Ma Bridge during Typhoon Sam was carried out between the computed results using the improved method and

those measured on the Bridge. The comparison was found satisfactory in general.

To have a deep understanding of skew wind effects and a higher confidence of the improved method for buffeting analysis, extensive parametric studies are being conducted by taking the Tsing Ma suspension bridge as a background. The preliminary results show that within a range of wind yaw angles ($\pm 30^\circ$) and wind inclinations ($\pm 5^\circ$), the maximum displacement response of the bridge deck occurs at about $\pm 30^\circ$ (yaw angle) and 4° (inclination) in the vertical direction, about 5° (yaw angle) and -2° (inclination) in the lateral direction, and about 0° (yaw angle) and -2° (inclination) in the torsional direction.

It should be pointed out that in this study, some key information regarding the modeling of aerodynamic forces such as admittance functions was not quantified through wind tunnel tests for the Tsing Ma Bridge. The field measurement data regarding wind characteristics were not comprehensive, such as the lack of spatial correlation of turbulent winds. Thus, more field measurements with improved monitoring systems and more comparisons having measured aerodynamic admittance functions should be carried out in the future. Furthermore, for demonstrating the utility of the proposed analytical framework, comparison with buffeting response of a scaled aeroelastic bridge model under simulated skew wind conditions in a wind tunnel will be carried out in near future.

Acknowledgements

The work described in this paper was financially supported by the Research Grants Council of Hong Kong (Project No. PolyU 5027/98E) to the first writer and The Hong Kong Polytechnic University through a PhD studentship to the second writer. The work is also part of a research project financially supported by the National Natural Science Foundation of China (Grant 59895410). Sincere thanks should go to the Tsing Ma Control Area Division of Hong Kong Highways Department for providing the writers with the design drawings. The writers also want to thank Ms J. Y. Xu, Mr Q. S. Ding, Mr. L. Zhao, Z. Prof. X. Lin, Mr J. Z. Song, Prof. A. R. Chen and Prof. Y. J. Ge of the State Key Laboratory for Disaster Reduction in Civil Engineering at Tongji University for their kind help during the wind tunnel tests. Thanks are also due to the anonymous reviewer who made valuable suggestions for the further study in this subject. Any opinions and concluding remarks presented in this paper are entirely those of the writers.

References

- Chen, J. and Xu, Y.L. (2002), "Identification of modal damping ratios of structures with closely spaced modal frequencies: HHT method", *J. Struct. Eng. Mech.*, **14**(4), 417-434.
- Davenport, A.G. (1962), "Buffeting of a suspension bridge by storm winds", *J. of Struct. Div., ASCE*, **88**(ST3), 233-268.
- Gu, M., Zhang, R.X., and Xiang, H.F. (2000), "Identification of flutter derivatives of bridge decks", *J. of Wind Eng. Ind. Aerodyn.*, **84**(2), 151-162.
- Jones, N.P., Scanlan, R.H., Jain, A., and Katsuchi, H. (1998), "Advances (and challenges) in the prediction of long-span bridge response to wind", *Bridge Aerodynamics*, Larsen & Esdahl (eds), Balkema, Rotterdam, The Netherlands, 59-85.
- Katsuchi, H., Jones, N.P., and Scanlan, R.H. (1999), "Multimode coupled flutter and buffeting analysis of the Akashi-Kaikyo bridge", *J. Struct. Eng., ASCE*, **125**(1), 60-70.
- Kimura, K. and Tanaka, H. (1992), "Bridge buffeting due to wind with yaw angles", *J. Wind Eng. Ind. Aerodyn.*,

41-44, 1309-1320.

- Lau, C.K., Wong, K.Y. and Chan, K.W.Y. (1998), "Preliminary monitoring results of Tsing Ma Bridge", *The 14th National Conf. on Bridge Eng.*, Shanghai, **2**, 730-740.
- Scanlan, R.H. (1999), "Estimates of skew wind speeds for bridge flutter", *J. Bridge Eng. ASCE*, **4**(2), 95-98.
- Scanlan, R.H. and Gade, R.H. (1977), "Motion of suspended bridge spans under gusty wind", *J. Struct. Div., ASCE*, **103**, 1867-1883.
- Simiu E. and Scanlan R.H. (1996), *Wind Effects on Structures*, John Wiley & Sons, INC, New York.
- Tanaka, H. and Davenport, A.G. (1982), "Response of taut strip models to turbulent wind", *J. Eng. Mech., ASCE*, **108**(1), 33-49.
- Sun, D.K., Xu, Y.L., Ko, J.M., and Lin, J.H. (1999), "Fully coupled buffeting analysis of long span cable-supported bridges: formulation", *J. Sound and Vib.*, **228**(3), 569-588.
- Vickery B.J. (1966), "Fluctuating lift and drag on a long cylinder of square cross-section in a smooth and in a turbulent stream", *J. Fluid Mech.*, **25** Part 3, 481-494.
- Xie, J. and Tanaka, H. (1991), "Buffeting analysis of long span bridges to turbulent wind with yaw angles", *J. Wind Eng. Ind. Aerodyn.*, **37**(1), 65-77.
- Xu, Y.L., Ko, J.M., and Zhang W.S. (1997), "Vibration studies of Tsing Ma Suspension Bridge", *J. of Bridge Eng. ASCE*, **2**(4), 149-156.
- Xu, Y.L., Zhu, L.D., Wong, K.Y., and Chan, K.W.Y. (2000a), "Field measurement results of Tsing Ma suspension bridge during Typhoon Victor", *J. Struct. Eng. Mech.*, **10**(6), 454-559.
- Xu, Y.L., Sun, D.K., Ko, J.M., and Lin, J.H. (2000b), "Fully-coupled buffeting analysis of Tsing Ma suspension bridge", *J. Wind Eng. Ind. Aerodyn.*, **85**(1), 97-117.
- Zhu, L.D., Xu, Y.L., Zhang, F., and Xiang, H.F. (2002a), "Tsing Ma bridge deck under skew winds. I: aerodynamic coefficients", *J. Wind Eng. Ind. Aerodyn.*, **90**(7), 781-805.
- Zhu, L.D., Xu, Y.L., and Xiang, H.F. (2002b), "Tsing Ma bridge deck under skew winds. II: flutter derivatives", *J. Wind Eng. Ind. Aerodyn.*, **90**(7), 807-837.

CC